J. RYBA[1], M. KAWALEC[1], E. TYRAŁA[1], H. KRAWIEC[1*]

EFFECT OF THERMAL TREATMENT OF BIOMEDICAL Ti-6Al-4V ALLOY ON CORROSION RESISTANCE IN SIMULATED PHYSIOLOGICAL SOLUTIONS

The effect of heat treatment on the corrosion resistance of Ti-6Al-4V alloy was investigated in the artificial saliva solution (MAS). It has been revealed that the thermal annealing treatment temperature favors the cathodic reactions and reduce the protective properties of passive film. The heat treatment causes the enrichment of β phase in vanadium. The lowest corrosion resistance in the artificial saliva revealed the Ti-6Al-4V alloy heated for 2 hours at 950°C. Heterogeneous distribution of vanadium within the β phase decreases the corrosion resistance of the Ti-6Al-4V.

Keywords: titanium alloys, corrosion, heat treatment, microstructure

1. Introduction

Nowadays, the most commonly used metallic materials in medicine are titanium alloys, in particular the Ti-6Al-4V alloy. This alloy has the following properties: very good biocompatibility, very good corrosion resistance, the highest biotolerance, low density ($4.30 \div 4.85$ g/cm^3), high fatigue strength and very good paramagnetic properties. Thanks to the above properties, this alloy has been used in the production of long-term internal orthopedic implants (prostheses and endoprostheses) and dental implants [1-4].

The Ti-6Al-4V alloy is classified as two-phases ($\alpha + \beta$) alloy, in which the α-phase is stabilized by aluminum and the β-phase is stabilized by vanadium present in the alloy. The microstructure of the Ti-6Al-4V alloy consists mainly (at room temperature) with hexagonal closed packed (HCP) for α and body cantered cubic (BCC) for β phases, respectively [5,7].

Corrosion resistance of biomedical titanium alloys results from the presence of a passive layer spontaneously formed on their surface. In the case of commercial Ti-6Al-4V, the passive layer on its surface consists mainly of titanium dioxide (TiO$_2$). Some experiments have shown that the amount of titanium dioxide increases with the value of applied potential [7]. In addition, the passive layer consists of small amount of aluminum oxide (Al$_2$O$_3$) and vanadium oxide (V$_2$O$_3$) [6]. There are also other oxides in the internal interface metal / oxide layer, such as TiO

and Ti$_2$O$_3$. The titanium implants stay in the body for more than 15 years, so at this time the passive layer can be hydrolyzed due to interaction with the body fluid. It is believed that Al^{3+} ions affect Alzheimer's disease and vanadium oxide is carcinogenic [8-11]. Therefore, the release of these elements to the body fluids can be danger for health.

Heat treatment of Ti alloys is one of ways, which allows to change their microstructure. Such changes sometimes reduce the amount of the pathogenic aluminum or other elements which are released to the body fluids during the corrosion [6,14]. Heat treatment of titanium alloys covers all processes which occur during the heating and cooling, which cause the phase transformations, segregation of alloying elements ect. [7,12]. Appropriately selected for each alloy heat treatment, allows to obtain the desired microstructure. For single-phase β alloys, the effect of thermal modification and strengthening is less noticeable, because it has a very high proportion of the β phase, which slows down the aging process and secretion strengthening [11].

The microstructure of titanium alloys is very important because the shape, number and size of grains affect the properties of the alloy. For example, in order to obtain $\alpha + \beta$ titanium alloy, the sample must be heated at a temperature below the phase transition temperature (eutectic) for several hours. Some specific features of microstructure of dual phases alloys are emphasized, such as irregular grain shape, discontinuous and continuous phase α at the grain boundary, and many secondary
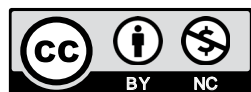
α phases. Intergranular regions may exist in a spherical, flaky or short α phase [8]. If the heat treatment proceeds at a higher temperature than the phase transition, the two existing faces will become a unique β phase. In order to improve the mechanical properties, and more specifically fatigue and tensile strength, the metal aging can be performed. When the β phase increases, the strengthening effect decreases, so the metastable β phase is aging and the α phase decreases. Ti-6Al-4V is a dual phases alloy, so in order to improve the shape of grains as well as global properties, this alloy must be subjected to aging treatment [5,11].

In this paper, the effect of thermal annealing treatment temperature on corrosion resistance of Ti-6Al-4V is studied in the artificial saliva solution (MAS – Mayer Artificial Saliva Solution).

2. Experimental

2.1. Materials and specimen preparation

The corrosion tests were carried out on Ti-6Al-4V alloys before and after heat treatment. The specimen after heat treatment were marked as: Ti-6Al-4V_HT_950 and Ti-6Al-4V_HT_950+500. The heat treatment was carried out in an oven in which the sample marked as Ti-6Al-4V_HT_950 was heated at 950°C for 2 hours, then it was cool down into a water to room temperature. The specimen marked as Ti-6Al-4V_HT_950 + 500 was heated at 950°C for 2 hours, cool down to 500°C temperature, then kept at this temperature for 4 hours and then cool down in air to room temperature. Before the corrosion tests, the all samples were mechanically smoothed using silicon carbide papers (SiC) to 4000 grades and polished using a colloidal silica (SiO_2) suspension. Between each step the samples were cleaned with ultrasound in ethanol.

In order to reveal the microstructure of Ti alloys tested before and after heat treatment, the polished samples were immersed in a Kroll's solution for 6 seconds and then washed with distilled water. The chemical composition of Kroll's solution is given in Table 1.

TABLE 1

The chemical composition of the Kroll's solution used for the chemical etching of titanium alloys [13]

Chemical compound	HNO$_3$	HF	H$_2$O
Quantity [ml]	6	3	100

The microstructure of tested Ti-6Al-4V alloy samples before and after heat treatment was observed by using Scanning Electron Microscopy SEM / EDS (JEOL JSM-5500LV). The hardness of Ti alloys was measured by the Vickers method. Vickers hardness (HV30) was measured at a load of 294.2 N. The hardness of specimens was 330 HV30 for Ti-6Al-4V (alloy before heat treatment), 427 HV30 for Ti-6Al-4V_HT_950, 454 HV30 for Ti-6Al-4V_HT_950+500, respectively.

2.2. Corrosion tests

Corrosion tests were carried out for all sets of samples (before and after heat treatment) in artificial saliva solution (MAS). The chemical composition of the artificial saliva solution (MAS) is given in Table 2. Corrosion measurements were made using a standard three-electrode electrolytic cell in which the following electrodes were placed: Ti-6Al-4V alloy – working electrode, Ag / AgCl (3M KCl) – reference electrode and Pt – counter electrode. Electrochemical measurements were carried out using the Autolab PGSTAT128 potentiostat. The following measurements were carried out in MAS at 37 °C: OCP – open circuit solution measurements, LSV – linear sweep voltamperometry and EIS – electrochemical impedance spectroscopy. The polarization curves (LSV) were plotted from –1000 mV vs. Ag / AgCl up to +2000 mV vs. Ag / AgCl at a potential scan rate of 1 mV s^{-1}. The electrochemical impedance spectra (EIS) were then plotted in the frequency range from 100 kHz to several mHz (70 points) using 10 mV peak-peak potential difference. The EIS spectra were determined at potentials located in the passive range at 0.5 V measured against the Ag / AgCl reference electrode (3M KCl).

TABLE 2

Chemical composition of artificial saliva (MAS) [15]

Chemical compound	Saliva solution (MAS) g/ dm^3 of H$_2$O
NaCl	0.7
KCl	1.2
NaHCO$_3$	1.5
Na$_2$HPO$_4$	0.26
KSCN	0.3
Na$_2$S × 9 H$_2$O	0.005
Urea	1.0

3. Results and discussion

3.1. Microstructure of Ti-6Al-4V alloy before and after heat treatment

Fig. 1 shows the microstructure of Ti-6Al-4V alloy before the heat treatment. The microstructure of this alloy consist of two phases: α and β. In Fig. 2, the microstructure of Ti-6Al-4V after heat treatments is presented. The microstructure revealed for the specimen Ti-6Al-4V_950 after etching in the Kroll's solution is presented in Fig. 2(a,c), while for the specimen Ti-6Al-4V_950 + 500 in the Fig. 2(b,d), respectively.

The results presented in Table 3 show the chemical composition of α and β phases for the tested specimens of Ti-6Al-4V alloy (before and after heat treatment). These values are calculated as an average value from 8 measurements. The EDS spectra obtained from the chemical analysis of the palaces are presented in Fig. 3. In the case of Ti-6Al-4V alloys subjected to heat treatment, phase β is depleted in vanadium, Fig. 2, Table 3. The chemical composition of the α phase for the specimens of Ti-6Al-4V alloy before

and after heat treatment is very similar. It should be notice that for the specimen Ti-6Al-4V_HT_950, some part of the β phase contains very low amount of vanadium (less than 1 at.%) and other part of this phase contains about 3 at.% of vanadium, (Table 3). Moreover, in the specimen Ti-6Al-4V_HT_950, β phase is enriched in aluminium compare to the specimen of Ti-6Al-4V alloy before the heat treatment. In the previous work [14] it has been shown that the heat treatme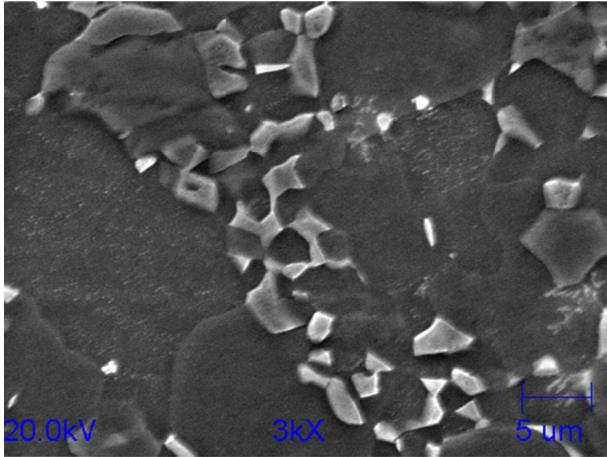nt process causes the preferential diffusion of vanadium in the β phase. In the case of specimen Ti-6Al-4V_HT_950 not uniform distribution of vanadium was detected. Such micro-segregation of vanadium in the Ti-6Al-4V alloy affects it corrosion resistance and the structure of passive layer. Moreover, this segregation of vanadium within β phase can cause the formation of micro-galvanic couplings at the surface of Ti-6Al-4V alloy which is in the contact with an electrolyte.

Fig. 1. Microstructure of Ti-6Al-4V alloy revealed after chemical etching in the Kroll's solution

TABLE 3

Chemical composition (at.%) of α and β phases before and after heat treatment of Ti-6Al-4V alloy. Investigated places are marked in the Fig. 1 and Fig. 2(a-d)

	Ti-6Al-4V			Ti-6Al-4V_ HT_950			Ti-6Al-4V_ HT_950 + 500		
	Ti	Al	V	Ti	Al	V	Ti	Al	V
α phase	88.0	10.5	1.5	87.0	11.0	1.3	89.0	10.0	1.0
β phase	86.0	8.0	**6.0**	88.0	11.4	**0.6**	88.0	8.0	**4.0**
β phase places 2, Fig. 2(b)				88.4	9.3	*2.8*			

Fig. 3 shows the EDS spectra of the intensity of analyzed elements in the chosen areas for the Ti-6Al-4V_HT_950 and for the Ti-6Al-4V_HT_950 + 500. The areas where the chemical analysis was performed are presented in the Fig. 2 (b,d).
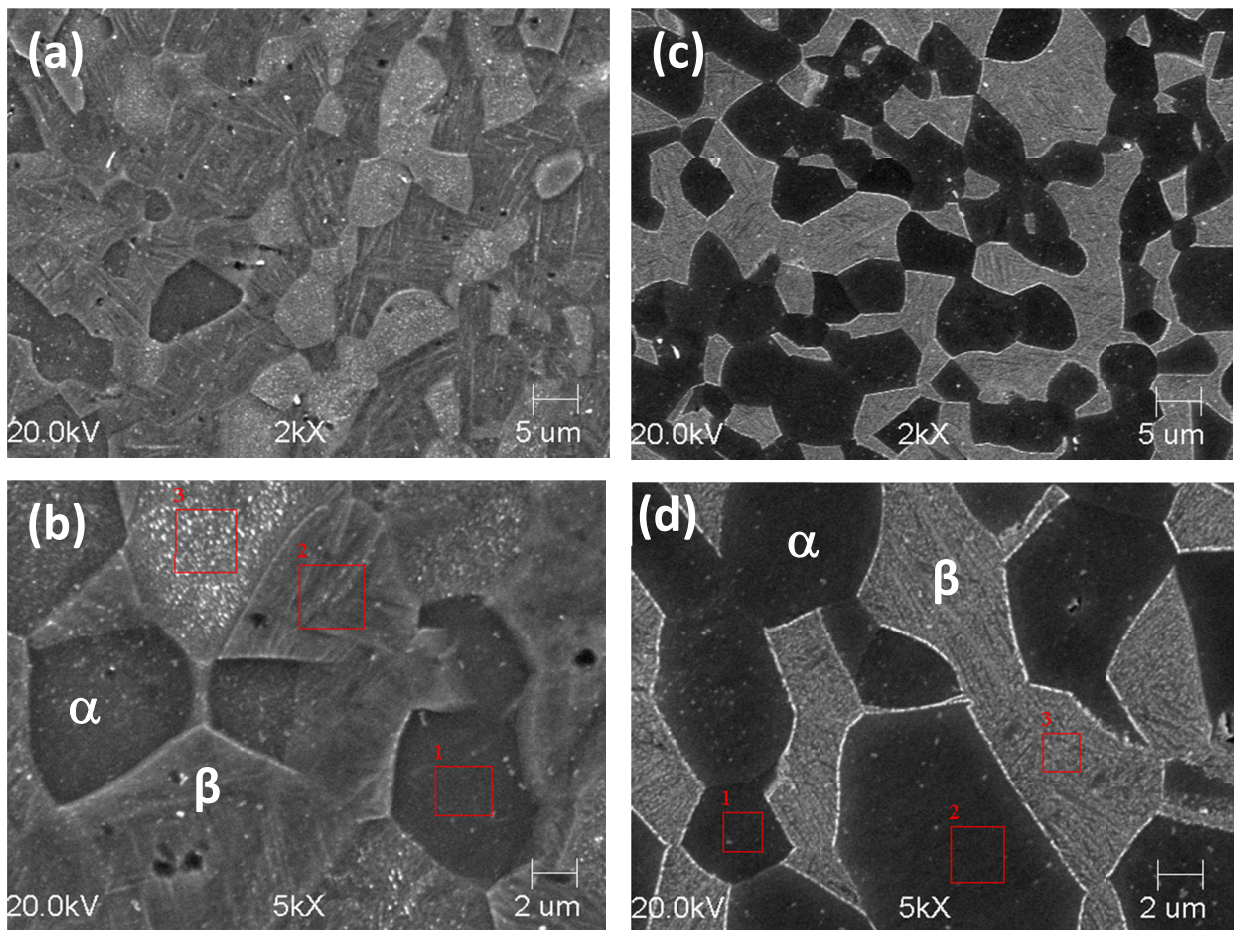

Fig. 2. Microstructure of Ti-6Al-4V specimens revealed after chemical etching in the Kroll's solution. Figures (a,b) for the Ti-6Al-4V_HT_950 and (c,d) for the Ti-6Al-4V_HT_950 + 500, respectively
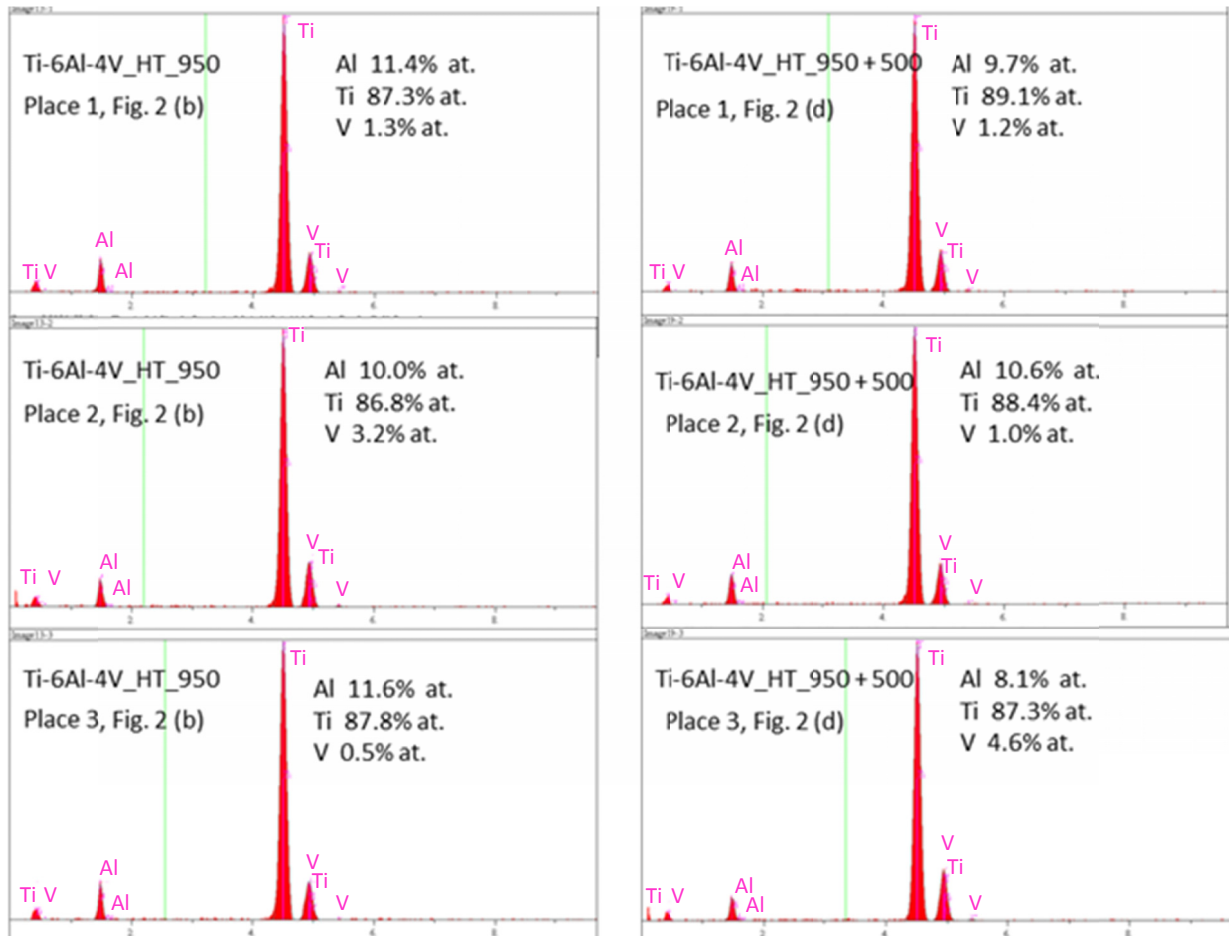
Fig. 3. EDS spectra obtained from the chemical analysis of the palaces marked in the figure 2(b,d)

3.2. Corrosion behavior of Ti-6Al-4V before and after heat treatment

Fig. 4(a) shows the evolution of open circuit potential (OCP) as a function of immersion time measured for titanium alloys in the artificial saliva. OCP increases and after 24 hours the following values are measured: –457 mV, –448 mV, –150 mV against Ag / AgCl (3 M KCl) for Ti-6Al-4V_HT_950, Ti-6Al-4V_HT_950 + 500 and Ti-6Al-4V, respectively.

The difference around 300 mV in OCP values between the Ti alloy before and after heat treatment suggests, that the tested Ti-specimens sets should have different corrosion resistance.

The polarization curves (LSV) revealed that cathodic current density measured for heat treated titanium alloys is much higher that this one measured for Ti-6Al-4V alloy before heat treatment, Fig. 4(b). Such results indicate that the cathodic reaction (reduction of oxygen) is favored on the surface of heat treated Ti alloy. The oxygen reduction occurring in the cathodic
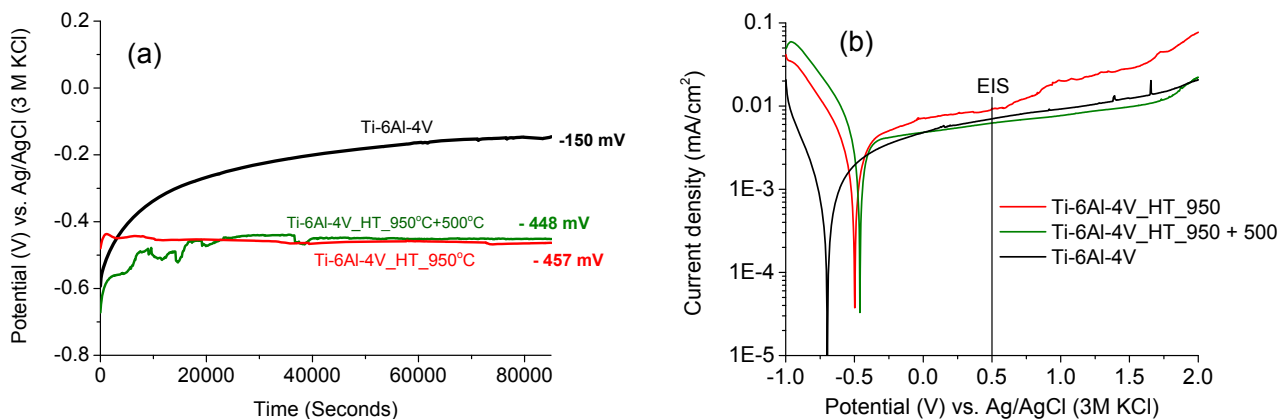

Fig. 4. The evolution of open circuit potential (a) and potentiodynamic polarization curves (b) obtained for Ti-6Al-4V and Ti-6Al-4V_HT specimens in artificial saliva at 37°C

domain causes the local alkalization of solution near the surface of sample. In the anodic branch a large passive range is observed for all Ti-6Al-4V specimens. The current density recorded for samples without heat treatment Ti-6Al-4V and after heat treatment marked as a Ti-6Al-4V_HT_950 + 500 is similar (curves: green and black Fig. 4(b)). The most active corrosion behaviour exhibits the specimens of Ti-6Al-4V alloy previously heated at 950°C for 2 hours and then quench in a water (red curve, Fig. 4(b)).

In order to check how the type of the heat treatment affects the corrosion resistance, Ti-6Al-4V_HT_950 and Ti-6Al-4V_HT_950 + 500 alloys were immersed for 6 days in the artificial saliva solution. Fig. 5 depicts the images of surface after corrosion tests. Observation of surface of Ti-6Al-4V_HT_950 after corrosion, (Fig. 5a,b), revealed the presence of the following places: black area (place 3, Fig. 5(b)), white area (place 1, Fig. 5(b)) and grey (place 2, Fig. 5(b)). EDS analysis has revealed the difference in the chemical composition of these places. Black and white areas contain mainly titanium (~78 at.%), aluminium (~10 at.%), vanadium (~4 at.%) and oxygen* (~10 at.%, * – from stoichiometric calculation). However, the grey area does not contains oxygen, but contains titanium (~84 at.%), aluminium (~10 at.%) and vanadium (~3 at.%).

It should be notice that the black small area (pits) are formed at the interfaces α/β (grey / white) or inside the β phase, Fig 5(a,b). Chemical composition of the characteristic places present on the surface of Ti-6Al-4V_HT_950 + 500 specimen (Fig. 5(c,d)) has revealed the similar chemical composition for the black areas, while others areas are not oxidized. The content of oxygen in the white, grey areas was below 3 at. %, and the content of titanium was ~85 at.%, vanadium (~3 at.%), aluminium (~10 at. %). These results confirm that the specimen Ti-6Al-4V_HT_950 slightly easier undergoes to oxidized in the artificial saliva than the Ti-6Al-4V_HT_950 + 500 specimen.

3.3. Passive properties of Ti-6Al-4V alloy before and after heat treatment

In order to test the resistance of passive film formed at the surface of Ti-6Al-4V samples before and after heat treatment Ti-6Al-4V_HT_950 and Ti-6Al-4V_HT_950 + 500, electrochemical impedance measurements were carried out in the artificial saliva. The EIS spectra were plotted under potentiostatic conditions at a constant potential of 0.5 V against Ag / AgCl (3 M KCl). This potential is located in the passive range as it is shown in the Fig. 4(b). Fig. 6 shows the Bode diagrams obtained for Ti-6Al-4V alloys before and after heat treatment. The symbols present the experimental points, and the lines present the data obtained from the fitting of electrical equivalent circuit (EEC).
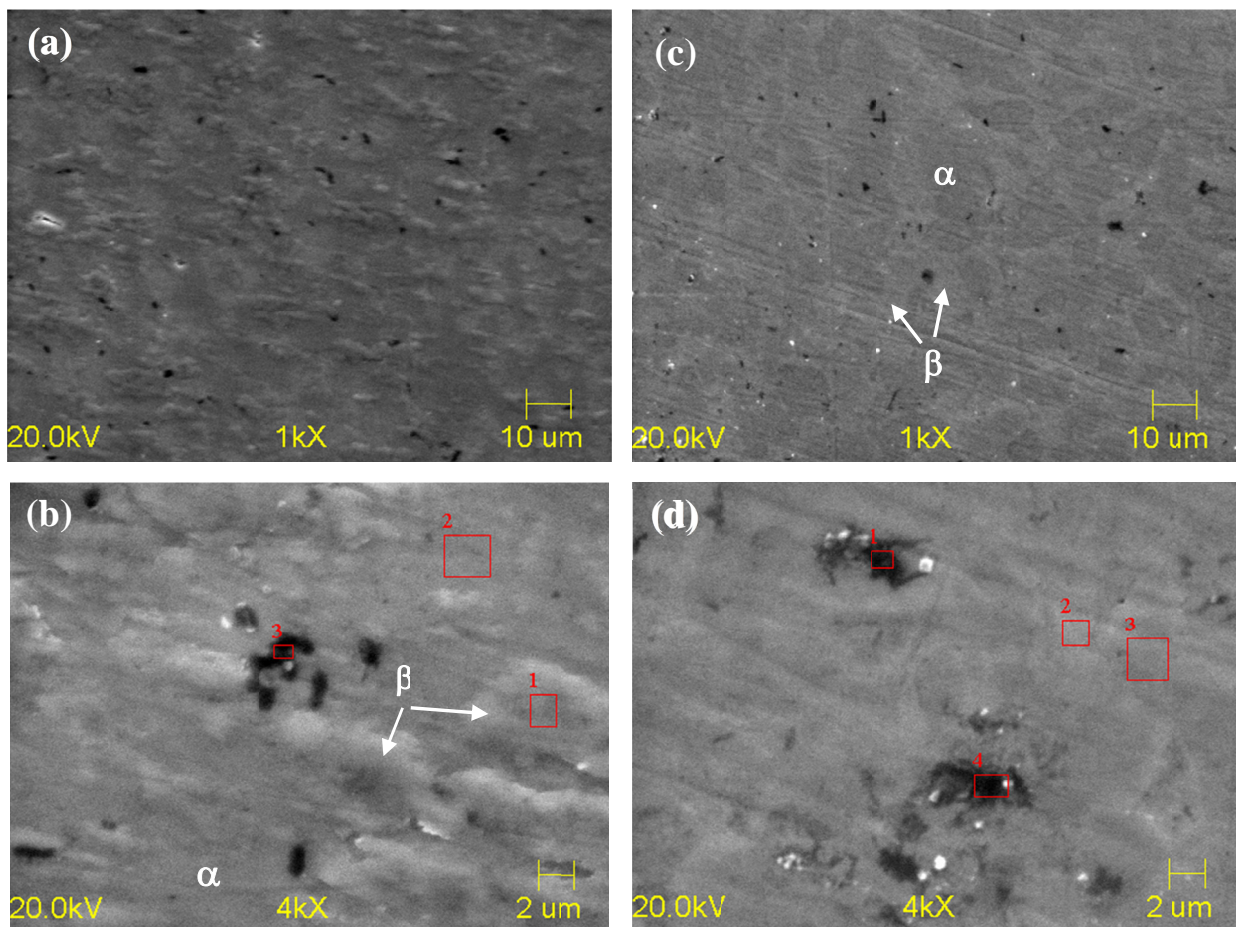

Fig. 5. SEM/EDS images registered for Ti-6Al-4V_HT_950 (a,b) and Ti-6Al-4V_HT_950 + 500 (c,d) after 6 days immersion at OCP in the solution of artificial saliva
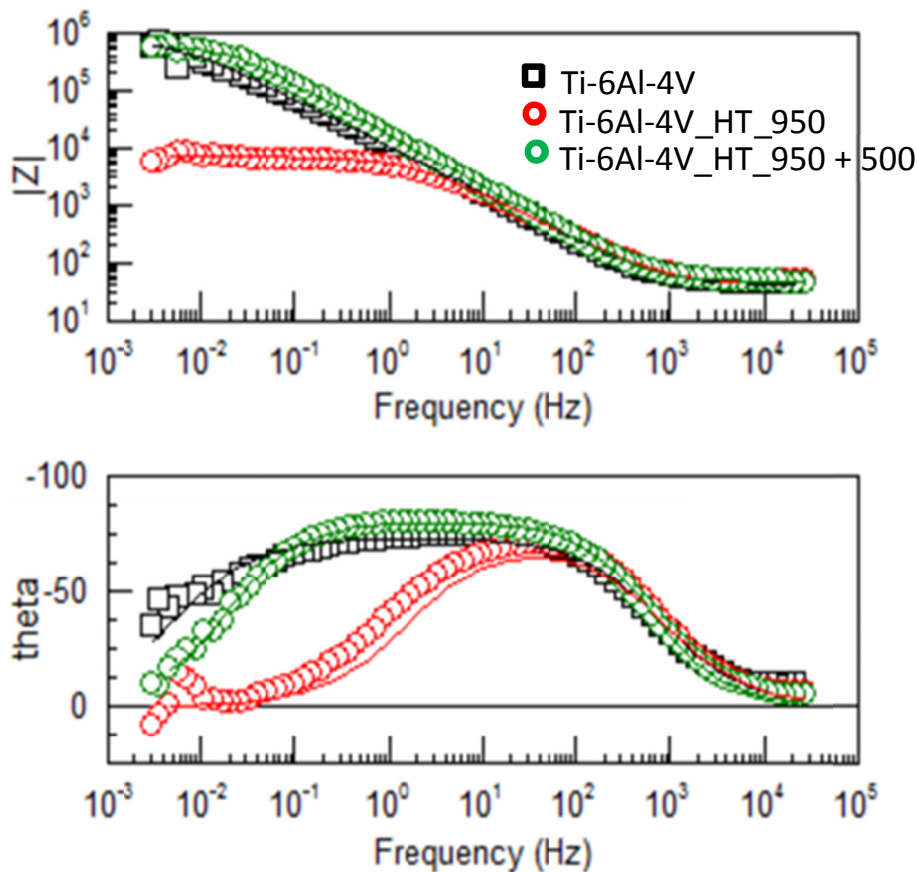
Fig. 6. Bode diagrams plotted for Ti-6Al-4V and Ti-6Al-4V_HT specimens in the artificial saliva at 0.5 V vs. Ag/AgCl (3M KCl). The symbols present the experimental points, and the lines present the data obtained from the fitting of electrical equivalent circuit

The electrical circuit which was used for fitting the experimental spectra is presented in Fig. 7. In the electrical equivalent circuit the following elements are present: R1 – electrolyte resistance, CPE – phase constant element, R2 – resistance of the passive film. All spectra exhibit one capacitive loop, Fig. 6. The passive film formed on the surface of Ti-6Al-4V exhibits the capacitive properties, the parameter CPE1-P is between 0.8 and 0.9, Table 4. The lowest resistance of passive film was obtained for the specimen Ti-6Al-4V_HT_950 (black symbols, Fig. 6). However, as it was shown in the Table 4, that the highest resistance (R2) of oxide film formed at the specimen's surface was obtained for Ti-6Al-4V and Ti-6Al-4V_HT_950 + 500, Table 4. In the previous work [14] it was proved, that heat treatment of Ti-6Al-4V (heating at 900°C for 2 hours and water quenching) cause the enrichment of β phase in vanadium. This element is very active and easily undergoes the dissolution into the electrolyte (artificial saliva). In the case of the specimens Ti-6Al-4V_HT_950, the β phase is enriched in aluminium, Table 3. However, the distribution of vanadium in the β phase is not uniform in the specimen Ti-6Al-4V_HT_950, Table 3, Fig. 2(a,b). There are some parts of β phase where can find high amount of vanadium and elsewhere lower amount. Heterogeneous distribution of vanadium within one phase causes weakening of passive layer and accelerate the dissolution (oxidation) of Ti-6Al-4V_HT_950 alloy. Not uniform oxidation of Ti-6Al-4V_HT_950 surface in the artificial saliva has been confirmed by immersion tests, Fig. 5.
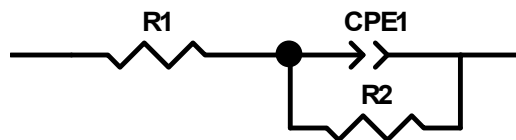

Fig. 7. Electrical equivalent circuit used for fitting the EIS spectra obtained for Ti-6Al-4V and for Ti-6Al-4V_HT at 0.5 V potential in the artificial saliva solution

TABLE 4

Values of parameters obtained from fitting the electrical equivalent circuit

	Ti-6Al-4V	Ti-6Al-4V_ HT_950	Ti-6Al-4V_ HT_950 + 500
R1 [Ω*cm^2]	41.5	43.2	47.2
R2 [Ω*cm^2]	805220	6957	606490
CPE1-T [Ω^{-1}cm^{-2}s^P]	$2.1*10^{-5}$	$2.1*10^{-5}$	$1.15*10^{-5}$
CPE1-P	0.82	0.80	0.90

The heat treatment is one of the methods which is used for the surface modification of Ti alloys and improvement of their mechanical properties and corrosion resistance. Some researchers have applied the Diamond Like Carbon (DLC) coatings [15] which allow to improve the resistance of Ti-6Al-4V alloy and 316L stainless steel to pitting, crevice and stress corrosion cracking. These type of coatings exhibit the amorphous nanocrystalline

structure and very good adherence to the metallic substrate. Very good wear resistance have revealed the nitride layer produced on the surface of Ti-6Al-4V alloy using glow discharge assisted nitriding process at the plasma potential [16]. Nitride layer formed on the surface of Ti-6Al-4V alloy consists of different sublayers in which the segregation of aluminium was determined [17]. During the plasma nitriding process, nitrogen diffusion into the metallic substrate lead to the depletion in aluminium of the upper part of the diffusive layer. Heterogeneous distribution of aluminium in the diffusive layer has impact on the corrosion resistance of Ti alloy. These results have shown that the heterogeneous distribution of alloying elements at the surface of alloy or within one phase slightly modifies the passive properties and corrosion behaviour of Ti-6Al-4V alloy.

4. Conclusions

Corrosion tests have been performed on Ti-6Al-4V alloy in the artificial saliva (MAS). The specimens of Ti-6Al-4V alloy before and after heat treatment were investigated. The following conclusions can be given:

1) The highest corrosion resistance revealed the Ti-6Al-4V and Ti-6Al-4V_HT_950 +500 specimens in the artificial saliva.

2) Heat treatment causes not uniform distribution of vanadium in the β phase.

3) Heating of Ti-6Al-4V at the 950°C for two hours then water quenching cause heterogeneous distribution of vanadium in β phase. This is the reason for the heterogeneous dissolution of Ti-6Al-4V_HT_950 alloy in the artificial saliva.

4) Heating of Ti-6Al-4V at the 950°C for two hours then ageing at 500°C for four hours significantly improve the passive properties of Ti alloy.

REFERENCES

[1] A. Łukaszewicz, M. Szota, Interational OCSCO World Press. **72**, 58-66 (2015).

[2] A. Bylica: J. Sieniawski, Tytan i jego stopy, Państwowe Wydawnictwo Naukowe, Warszawa (1985).

[3] C.C. Chen, J.H. Chen, C.G. Chao, W.C. Say. J. Mater. Sci. **40**, 4053-4059 (2005).

[4] A. Choubey, R. Balasubramaniam, B. Basu. Journal of Alloys and Compounds **381**, 288-294 (2004).

[5] J.C.M. Souza, P. Ponthiaux, M. Henriques, R. Oliveira, W. Teughels. Journal of Dentistry **41**, 528-34 (2013).

[6] B. Sivakumar. S. Kumar, S.N. Sankara Narayanan. Wear. **270**, 317-324 (2011).

[7] I. Gurappa. Mater. Charact. **49**, 73-79 (2002).

[8] P. Flores-Álvarez, J. Rodríguez-Gómez, E. Onofre-Bustamante, J. Genescá-Llongueras, Surface & Coatings Technology **315**, 498-508 (2017)

[9] J. Loch, H. Krawiec, A. Łukaszczyk, J. Augustyn-Pieniążek, Achievements in Materials and Manufacturing Engineering **74** (1), 29-30 (2016)

[10] M. Głowacka, Metaloznawstwo, Wydawnictwo Politechniki Gdańskiej, Gdańsk (1996).

[11] K. Oczoś, A. Kawalec, Kształtowanie metali lekkich, Wydawnictwo Naukowe PWN, Warszawa (2012).

[12] Z. Cai, T. Shafer, I. Watanabe, E.M. Nunn, T. Okabe, Biomaterials **24**, 213-218 (2003).

[13] H. Krawiec, V. Vignal, E. Schwarzenboeck, J. Banaś. Electrochimica Acta **104**, 400-406 (2013).

[14] J. Ryba, H. Krawiec, M. Kawalec, E. Tyrała. Ochrona przed korozją, **61**, 255-258 (2018).

[15] J. Marciniak, J. Szewczenko, W. Kajzer, Archives of Metallurgy nad Materials **60**, 2123-2129 (2015).

[16] M. Tarnowski, K. Kulikowski, T. Borowski, B. Rajchel, T. Wierzchoń, Diamond & Related Materials **75**, 123-130 (2017).

[17] J. Morgiel, T. Wierzchoń, Surface & Coatings Technology **259**, 473-482 (2014).